RESOURCES *for the* FUTURE

Impact of Solar Geoengineering on Temperature-Attributable Mortality

Anthony Harding, David Keith, Wenchang Yang, and Gabriel Vecchi

Working Paper 23-23
May 2023

About the Authors

Anthony Harding is a postdoctoral fellow researching the intersection of innovative technologies and climate policy. He received his PhD in economics from Georgia Institute of Technology, where his research focused on climate and energy economics, and earned a BS from Rensselaer Polytechnic Institute in math and physics. Harding's research applies both econometrics and economic modelling to evaluate climate policy and climate impacts. His most recent work estimates the distribution of economic impacts of solar geoengineering across countries and compares it to the impacts of climate change. His current interests include the design of effective international climate governance structures and the measurement of the value of scientific learning.

David Keith has worked near the interface between climate science, energy technology, and public policy for twenty-five years. He took first prize in Canada's national physics prize exam, won MIT's prize for excellence in experimental physics, and was one of TIME magazine's **Heroes of the Environment**. Keith is Professor of Applied Physics at the Harvard School of Engineering and Applied Sciences and Professor of Public Policy at the Harvard Kennedy School, and founder of **Carbon Engineering**, a company developing technology to capture CO_2 from ambient air to make carbon-neutral hydrocarbon fuels. Best known for his work on the science, technology, and public policy of solar geoengineering, Keith led the development of **Harvard's Solar Geoengineering Research Program**, a Harvard-wide interfaculty research initiative.

Wenchang Yang is an associate research scholar in the Department of Geosciences at Princeton University, working in the group of Prof. Gabriel Vecchi. His research is focused on better understanding climate variability and change on broad timescales from sub-seasons to millennia, as well as why the mean climate of the planet is the way it is.

Gabriel Vecchi is a professor of geosciences at **The High Meadows Environmental Institute**, and director of **Cooperative Institute for Modeling the Earth System** at Princeton University. His research interests are climate science; extreme weather events; hurricanes; mechanisms of precipitation variability and change; ocean-atmosphere interaction; detection and attribution.

Acknowledgments

Anthony Harding and David Keith acknowledge support from the LAD Climate Fund. Gabriel Vecchi and Wenchang Yang acknowledge support from US Department of Energy Grant DE-SC0021333. We thank Kevin Cromar and other participants in workshops at Resources for the Future for useful comments and feedback. We thank Simone Tilmes for assistance in accessing GLENS simulation data. We thank Antonella Zanobetti and Joel Schwartz for helpful conversations in the early stages of the project.

About RFF

Resources for the Future (RFF) is an independent, nonprofit research institution in Washington, DC. Its mission is to improve environmental, energy, and natural resource decisions through impartial economic research and policy engagement. RFF is committed to being the most widely trusted source of research insights and policy solutions leading to a healthy environment and a thriving economy.

Working papers are research materials circulated by their authors for purposes of information and discussion. They have not necessarily undergone formal peer review. The views expressed here are those of the individual authors and may differ from those of other RFF experts, its officers, or its directors.

About the Project

The Resources for the Future Solar Geoengineering research project applies tools from multiple social science research disciplines to better understand the risks, potential benefits, and societal implications of solar geoengineering as a possible approach to help reduce climate risk alongside aggressive and necessary mitigation and adaptation efforts. The project began in 2020 with a series of expert workshops convened under the SRM Trans-Atlantic Dialogue. These meetings resulted in a 2021 article in *Science* that lays out a set of key social science research questions associated with solar geoengineering research and potential deployment. The Project followed this with additional sponsored research, including a competitive solicitation designed to address research areas highlighted in the *Science* article. This paper is one of eight research papers resulting from that competition and supported by two author workshops. A key goal of the solicitation and the overall project is to engage with a broader set of researchers from around the globe, a growing number of interested stakeholders, and the public.

Sharing Our Work

Abstract

Temperature-attributable mortality is a major risk of climate change. We analyze the capacity of solar geoengineering (SG) to reduce this risk and compare it to the impact of equivalent cooling from CO_2 emissions reductions. We use the Forecast-Oriented Low Ocean Resolution model to simulate climate response to SG. Using empirical estimates of the historical relationship between temperature and mortality from Carleton et al. (2022), we project global and regional temperature-attributable mortality, find that SG reduces it globally, and provide evidence that this impact is larger than for equivalent cooling from emissions reductions. At a regional scale, SG moderates the risk in a majority of regions but not everywhere. Finally, we find that the benefits of reduced temperature-attributable mortality considerably outweigh the direct human mortality risk of sulfate aerosol injection. These findings are robust to a variety of alternative assumptions about socioeconomics, adaptation, and SG implementation.

Contents

1. Introduction

Climate model analyses demonstrate wide accordance that solar geoengineering (SG) applied uniformly (balanced across hemispheres) and moderately (to offset less than half of the warming from greenhouse gases) moderates salient climate risks, such as extreme weather (Dagon and Schrag 2017; Irvine and Keith 2020), permafrost loss (Chen et al. 2020, 2022), and changes in crop yields (Fan et al. 2021). Yet, it also introduces novel risks. These include the direct risks from the aerosols used (Eastham et al. 2018), regional exacerbation of climate changes (Moreno-Cruz et al. 2012), and rapid and extreme warming if suddenly terminated (Parker and Irvine 2018). Decisions about SG should be informed by comprehensive and quantitative risk–risk (Harding et al. 2022; Felgenhauer et al. 2022; Parson 2021) analyses that weigh SG's capacity to moderate climate risks against the risks its use entails.

We take a small step toward a more comprehensive risk–risk analysis by estimating the impact of SG on temperature-attributable mortality—a major risk of climate change. A recent global-scale study (Carleton et al. 2022) finds that the mortality risk of climate change is around 85 deaths per 100,000 by the end of the 21st century for a high-warming scenario (14 for a moderate-warming scenario). In monetary terms, the study estimates that the mortality component of the social cost of carbon is $\$37/tCO_2$ ($\$17/tCO_2$ for a moderate-warming scenario). For comparison, the Interagency Working Group on Social Cost of Greenhouse Gases (2021) revised its estimates of the total social cost of carbon for use in regulatory impact analysis to $\$51/tCO_2$ in its February 2021 report. Another recent estimate of the social cost of carbon that incorporates temperature-attributable mortality risk finds that it is about half that cost (Rennert et al. 2020).

Despite the importance of mortality risk and growing interest in SG, research on its human mortality impact is scant. Eastham et al. (2018) quantify the impact of stratospheric sulfate aerosol on ground-level ozone, particulate matter, and ground-level UV-B flux and find a net mortality increase of 26,000 (95 percent CI: -30,000–79,000) deaths per year to reduce global mean temperatures by 1°C. Other research analyzes mortality from the effect on heat stress (Kuswanto et al. 2022) and malaria (Carlson et al. 2022) but does not quantify impacts.

Roughly uniform SG might employ a range of methods, from various stratospheric aerosols to cirrus thinning to space-based methods. The most technically feasible method is to add SO_2 to the stratosphere. Our judgment is that the most policy-relevant question for SG is how a moderate amount of it might supplement in a moderate emissions reduction scenario (e.g., to gradually achieve a peak reduction of 1°C in the latter half of the century). Given the uncertainty about technology and deployment strategy, our primary climate simulation uses solar constant reduction as a proxy for uniform SG. We explore the consequences of this choice by using an alternative simulation in which sulfate aerosol is injected with a control algorithm that tries to maintain multiple temperature targets.

We use the Geophysical Fluid Dynamics Laboratory Forecast-Oriented Low Ocean Resolution (FLOR) model to simulate climate changes (Vecchi et al. 2014) (see Methods). Relative to a 1990s control, we compare climate response over a 200-year experiment for doubling CO_2 concentrations ($2xCO_2$ experiment) and doubling CO_2 concentrations offset with a solar constant reduction of 1.7 percent ($2xCO_2$ +SG experiment). This solar constant reduction approximately offsets the change in top-of-atmosphere net radiative forcing from doubling CO_2 (Figure S1). FLOR has a spatial resolution of about 50km for land and atmosphere and 1°x1° for ocean and ice. We chose a model with a high spatial resolution because it improves accuracy in representing extreme weather (van der Wiel et al. 2016; Philip et al. 2021), which is particularly important in our setting. We use the final 100 years of each experiment to allow the climate system to equilibrate.

2. Results

2.1. Climate Response

If global average temperatures were the sole determinant of climate impacts, then SG might perfectly compensate for the climate impacts of CO_2. But impacts depend on local climate changes that cannot be eliminated by SG. A central technical question about SG is how much it exacerbates local climate changes—increasing their deviations from preindustrial. Because the amount of SG cooling is a policy choice, it is often most useful to compare the effects to those of identical global average cooling from reduced CO_2 concentrations. We introduce a ratio metric r_X that measures the effect of SG on a variable X normalized per degree global mean cooling *relative to* the effect of reducing CO_2 concentrations normalized per degree global mean cooling (see Methods), which could represent the effect of emissions reductions relative to a higher concentrations counterfactual or the effect of direct carbon removal. In the remainder of the paper, we refer to this as the "effect of emissions reductions." An $r_X > 1$ indicates that the response to SG is greater than the response to emissions reductions, and $r_X < 1$ indicates the response to SG is less than the response to emissions reductions.

We analyze the climate response to SG for dry-bulb temperature, the climate input variable for our empirically based analysis of temperature-attributable mortality. We consider the response of the annual means of temperature ($\overline{\mathrm{T}}$), intensity of consecutive hot days (T^{HW}), and intensity of consecutive cold days (T^{CW}) at the grid-cell level. The intensity of cold (heat) extremes are measured as the 10th (90th) percentile of the rolling five-day maximum (minimum) daily temperatures annually. The Supplementary Materials (Figures S2 and S3) present the results for other percentiles.

Figure 1. Temperature Response to Solar Geoengineering (SG) Relative to Emissions Reductions

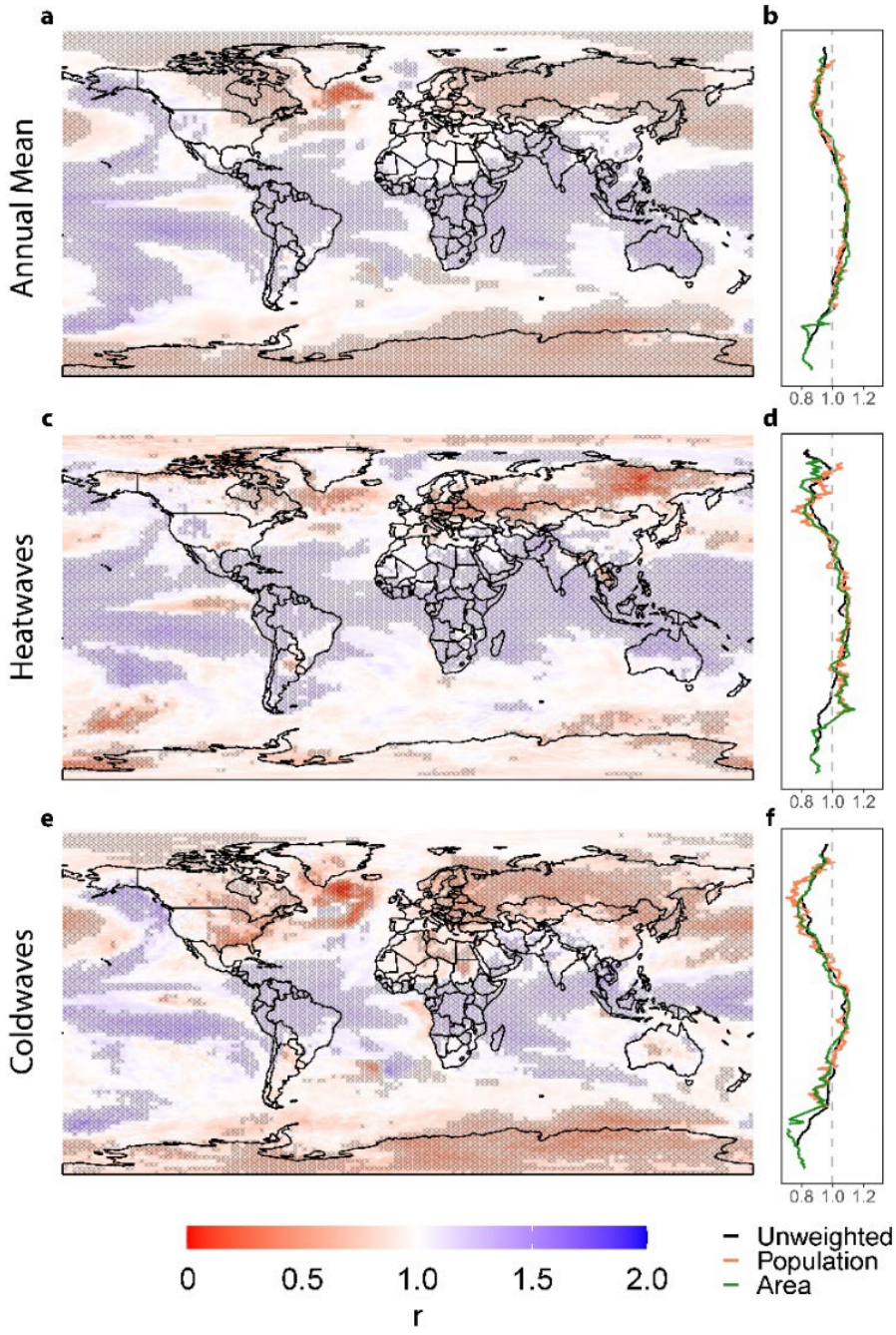

Left-hand subpanels show the ratio of the response of (a) annual mean temperature, (c) heatwave intensity, and (e) coldwave intensity per degree of cooling from SG relative to the response per degree of cooling from emissions reductions. Displayed values are the median over 100 climate simulation years. Blue (red) grid cells indicate SG reduces temperatures more (less) than emissions reductions. Crosshatches indicate statistical significance at 95 percent confidence level using a Wilcoxon signed-rank test corrected following the false discovery rate procedure. Right-hand subpanels show the zonal average of the left-hand subpanels for three weighting schemes.

Figure 1 shows the regional distribution of the estimated ratio metrics $r_{\bar{T}}$, $r_{T^{HW}}$, and $r_{T^{CW}}$. Perhaps the most striking characteristic is that compared to emissions reductions, per degree of global mean cooling, SG cools equatorial regions more and polar regions less. This dampening of the equator-to-pole gradient (or an overcooling of the tropics and undercooling of the poles) is a well-documented effect of globally uniform SG (Govindasamy and Caldeira 2000; Ban-Weiss and Caldeira 2010; Irvine 2016). It can be moderated through nonuniform SG that adjusts the latitudinal distribution of aerosol injection (Kravitz et al. 2019). Despite concern about tropical overcooling, uniform temperature reduction is objectively never the correct goal for SG. Given that a large fraction of the global population lives in equatorial regions, and the health and productivity impacts of additional warming are strongest in hot regions, utilitarian or justice concerns provide an argument for concentrating cooling in the tropics.

For each temperature metric, we calculate the global population-weighted mean, using population weights because we are concerned about changes relevant to human mortality. For annual average temperatures, the median global population-weighted mean $r_{\bar{T}}$ is 1.087 (95 percent CI: 1.066–1.11). This indicates that for equivalent average global cooling, SG cools annual mean temperatures by around 8.7 percent more than emissions reductions in the places people live. This is driven by an overcooling in the latitudinal bands of 30°N to 40°S, which is where a large fraction of the global population resides.

The response of heat extremes $r_{T^{HW}}$ is 1.086 (95 percent CI: 1.010–1.194), similar to that of annual mean temperatures both regionally and globally. Thus, SG tends to overcool the heat extremes in places people live more than emissions reductions does. This is consistent with analysis of its effect on heatwaves (Dagon and Schrag 2017). The change for cold extremes $r_{T^{CW}}$ is 1.045 (95 percent CI 0.967–1.167). We do not find a statistically significant difference in the global mean response to SG and emissions reductions. The respective zonal subplot in Figure 1 shows that SG leads to a relative overcooling of cold extremes in a much smaller latitudinal band range and undercools in more areas relative to annual means and heat extremes. Taken together, we find that SG reduces the intra-annual variability of temperatures in most populated regions (Figure S4). As temperature-attributable mortality is particularly sensitive to extremes, this is an important mechanism through which SG may differ from equivalent global cooling from emissions reductions.

2.2. Empirically Estimated Impact

We apply empirical estimates of the historical relationship between temperature and mortality to quantify the potential impact of SG at a global scale. Carleton et al. (2022) estimate the relationship between temperature and mortality rates using subnational data for 40 countries and capture a nonlinear exposure–response function with heterogeneity across age groups (<5, 5–64, >65) and across regions based on their historical climate and income (Figure ED1).

We follow the methodology outlined in Carleton et al. (2022) to extrapolate their empirical estimates and project temperature-attributable mortality for 24,378 regions spanning the globe, each around the size of a US county (see Methods). For our benchmark estimates, we assume income levels are consistent with Shared Socioeconomic Pathway 3 (SSP3) in 2015 and that people are adapted to 1990s climate. We account for uncertainty through Monte Carlo simulation, sampling across climate variability, and statistical uncertainty (see Methods).

Figures 2a–c show our estimate of the impact of SG on annual temperature-attributable mortality risk. We show the difference between temperature-attributable mortality in the $2xCO_2$ experiment and the $2xCO_2$+SG experiment normalized by the change in global mean temperatures. The risk is pooled across age groups within regions. Globally, we find that SG reduces temperature-attributable mortality by an average of 17 deaths per 100,000 per year per 1°C. For context, this is around 2.1 and 1.4 percent of the 2019 and projected end-of-century global all-cause mortality rate, respectively (UN 2022). Figure ED2a shows uncertainty in this estimate across Monte Carlo simulations; the majority of it is driven by uncertainty in the econometric estimates.

Figure 2. Impact of Solar Geoengineering (SG) on Temperature-Attributable Mortality

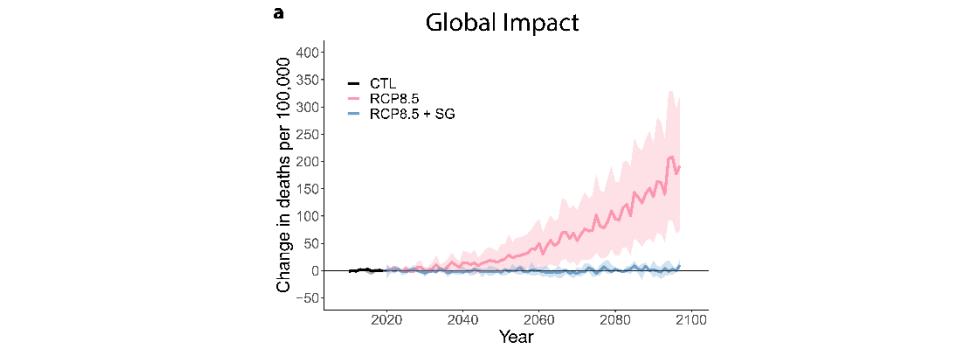

d

Impact of Solar Geoengineering								
	Decade							
Measure	2021-2029	2030-2039	2040-2049	2050-2059	2060-2069	2070-2079	2080-2089	2090-2097
$\Delta\bar{T}$ (°C)	0.2	0.7	1.4	2.2	2.7	3.3	4	4.8
SG (per 1°C)	0.1	8	12	14	22	24	30	36
r	1.14	1.03	1.2	1.09	1.18	1.09	1.06	1.04

Impact of solar geoengineering on temperature-attributable mortality rates by (a) population and (c) area. Difference in temperature-attributable mortality per degree of global mean cooling from emissions reductions and SG by (b) population and (d) area. Plots display median estimate across Monte Carlo simulation; (e) fraction of global population with positive or negative impact.

Impacts across both regions and age groups are heterogeneous. Some regions benefit from cooling, but others are harmed. Many regions of the Global South benefit, but mortality risk increases in many regions of the Global North. For example, per degree of cooling with SG, mortality risk in Boston, US *increases* by an average of 3 deaths per 100,000 per year while mortality risk in Mumbai, India *decreases* by an average of 12 deaths per 100,000 per year. Taking the median across Monte Carlo simulations, we find that 68 percent of the global population benefit from a reduction in mortality risk with solar geoengineering and 32 percent of the global population experience an increase in mortality risk. This benefit is strongest for the poorest regions (Figure ED3). Because the oldest age group (65+) is the most sensitive to temperature-attributable mortality (Figure ED1), it is the majority of both global and regional impacts, followed by the lowest age group (<5).

Figures 2b–d show the normalized impact of SG on temperature-attributable mortality relative to that of emissions reductions; we calculate the global ratio metric r_M as this ratio and estimate it as 1.12. This indicates that SG reduces temperature-attributable mortality by around 12 percent more than emissions reductions per degree of global mean cooling. This ratio is consistent across age groups, although, again, most of the level difference in risk is in the oldest age group. Figure ED2b shows uncertainty in this estimate across Monte Carlo simulations.

Much of the regional heterogeneity in SG's impact relative to emissions reductions can be explained by the heterogeneity in climate response and whether regions are made better or worse off with global cooling. This is made clear by decomposing mortality risk impacts into heat- and cold-attributable mortality. Generally, equatorial regions that benefit from cooling are better off with SG because it overcools them relative to emissions reductions (Figure ED4a). In the Global North, regions are generally worse off with cooling from SG because it overcools them relative to emissions reductions (Figure ED4b). Equatorial regions see an increase in cold-attributable mortality risk with SG, but the benefits from reduced heat-attributable mortality risk are stronger. For temperature-attributable mortality, we find that 80% of the global population benefit more from cooling with SG while 20 percent benefit more from cooling with emissions reductions.

3. Limitations and Uncertainties

Our analysis is only as credible as our assumptions. We break down the limitations and uncertainties in our analysis into those stemming from the empirical estimates and their application and those from the climate simulations.

3.1. Empirical Estimates

Section 7 of Carleton et al. (2022) outlines the limitations of their methodology in detail. Arguably the most relevant limitation for our setting is that dry-bulb surface temperature is their only climate variable input. From a physiological perspective, it is well known that factors other than ambient temperatures—such as humidity and radiation—are also important determinants of human health, particularly for heat stress

(Buzan and Huber 2020). These factors will be captured in the model to the extent that they correlate with dry-bulb temperature, but these correlations will change with SG or climate change (Harding et al. 2020). For example, SG optimized to restore temperature changes will strongly reduce precipitation changes (Moreno-Cruz et al. 2012).

SG could be less effective at reducing temperature-attributable mortality than we find here if, for example, changes in other relevant environmental conditions increased physiological stress in a way we are unable to capture. Lacking an empirical model to quantify these effects, we analyze the climate response to SG for both wet-bulb temperature (WBT) and wet-bulb globe temperature (WBGT) at the surface, two composite measures of heat stress that consider humidity, wind speed, and radiative flux (see Methods).

Figure 3. Wet-bulb and wet-bulb globe temperature response to solar geoengineering (SG) relative to emissions cuts

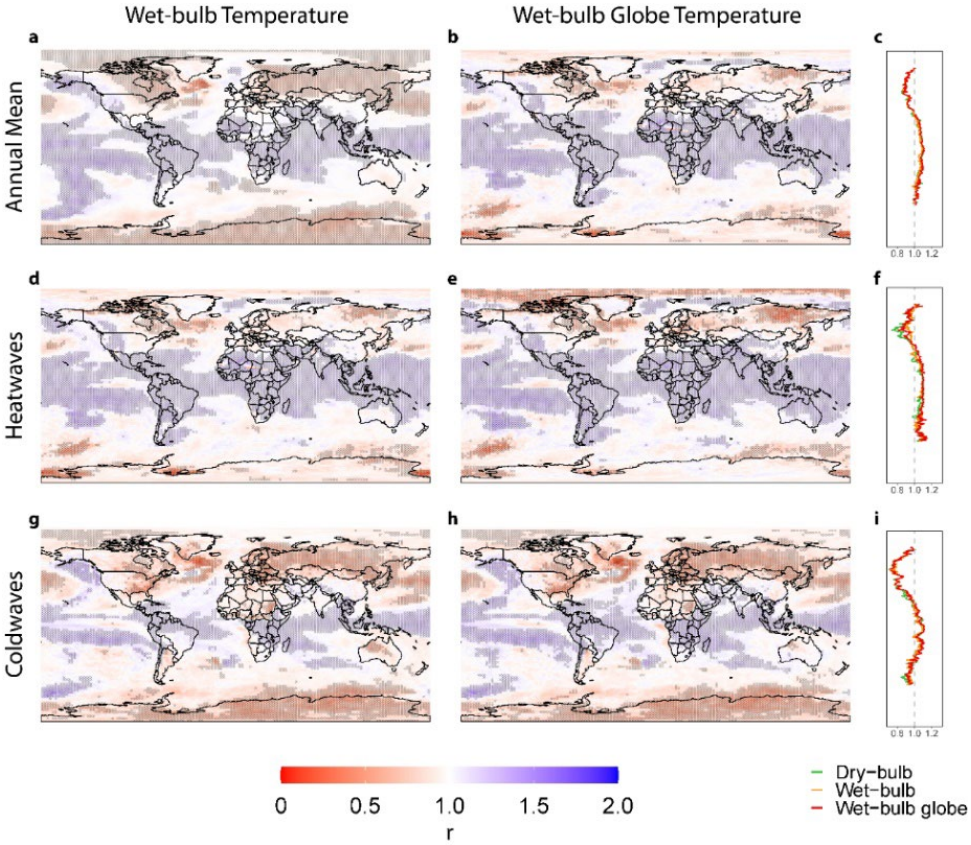

The left-hand and middle columns of subpanels show the ratio *r* of response for WBT and WGBT. These are estimated for annual mean temperature, heatwave intensity, and coldwave intensity per degree of cooling from SG relative to the response per degree of cooling from emissions reductions. Displayed values are the median over 100 climate simulation years. Blue grid cells indicate SG reduces temperatures more than emissions reductions and red grid cells indicate solar geoengineering reduces temperatures less. Crosshatches indicate statistical significance at the 95 percent confidence level using a Wilcoxon signed-rank test corrected following the false discovery rate procedure. Right-hand subpanels show the zonal population-weighted average for all three temperature metrics.

Figure 3 displays the ratio of the normalized response of both temperatures to SG relative to that of emissions reductions. Compared with Figure 1, the distribution of the response of both temperatures is similar to the response of dry-bulb temperature. The largest discrepancy is for heat extremes in northern regions, where the relative undercooling of SG is weaker. This raises the population-weighted average ratio $r_{T^{HW}}$ to 1.107 (95 percent CI: 1.063–1.132) for WBT and 1.122 (95 percent CI: 1.106–1.178) for WBGT. Consistency in the response of these more complex heat stress measures to the response of dry-bulb temperatures provide suggestive evidence that a more complex empirical model of temperature-attributable mortality will have similar findings as for dry-bulb temperature or perhaps even find SG to be more effective.

We assume that people have roughly present-day income levels and are adapted to near current-day climate when SG is deployed. However, that is unlikely for several decades (if at all). In that time, incomes will grow and people will adapt to a new climate. These changes will affect the impact on temperature-attributable mortality.

To constrain how much changes in these assumptions affect our findings, we re-estimate the projected impacts of SG under alternative assumptions. To constrain the role of income growth, we alternatively assume income levels given by SSP3 in 2080. To constrain the role of adaptation to changes in climate, we project mortality risk with perfect adaptation to the climate of each respective climate model experiment.

Allowing for income growth or perfect climate adaptation, we find that each reduces the global average impact on temperature-attributable mortality by 9 deaths per 100,000 per year per 1°C. We also estimate the impact relative to emissions reductions. Allowing for either income growth or climate adaptation yields a global ratio r_M of 1.12. Thus, alternative assumptions affect our estimate of the impact of SG on temperature-attributable mortality by around an order of 2x. However, changes in these assumptions have little effect on our estimates of how SG performs relative to emissions reductions.

The response of global temperature-attributable mortality is nonlinear in changes to global mean temperature. Thus, our normalization of the impacts of SG and emissions reductions, which linearizes the impact, may mechanically overstate the impact of SG because a 1.7 percent solar constant reduction typically does not fully restore the change in global mean temperature from a doubling of CO_2 concentrations. To check this, we estimate the impact of SG and emissions reductions using a subset of the final 100 simulation years. We consider the 47 years in which global mean temperatures overlap for the control and SG scenarios; we estimate the reduction in annual temperature-attributable mortality per degree of global mean cooling for SG is around 1.103 times that of emissions reductions, a small change from our unconstrained result. This indicates that the response nonlinearity is not driving our finding.

3.2. Climate Simulations

Any simulation of stratospheric aerosol SG carries two kinds of uncertainty. First is about policy choices—how much aerosol is deployed and how it is distributed. Given the strong effects of shifting the ITCZ, we assume that any stable deployment would aim at balancing between the northern and southern hemispheres. This still leaves a nonobvious policy choice about how much aerosol to deploy and how to address cooling the tropics versus the poles. Second, all climate models have substantial limitations, and model capabilities have trade-offs.

We use the FLOR model driven by a uniform solar constant reduction, which approximates what could be achieved with aerosol injection aimed at mimicking a uniform reduction, a choice that tends to cool the tropics a bit more strongly than the poles. The advantage of the FLOR model is that its higher spatial resolution and longer time horizon provide better representation of extremes. The disadvantage is that it does not treat the stratospheric impacts of sulfate aerosol, such as stratospheric heating (Visioni et al. 2021; Bednarz et al. 2022).

As an alternative, we use the Stratospheric Aerosol Geoengineering Large Ensemble project (GLENS) simulations, which are driven by stratospheric aerosol injection at four latitudes in a scheme that aims to maintain multiple temperature targets, including the equator–pole gradient (see Methods). The advantage is that the atmospheric component, Whole Atmosphere Community Climate Model (WACCM), has a high-quality representation of stratospheric dynamics. A disadvantage is that lower resolution and shorter integration time limit the ability to model changes in extremes.

We project temperature-attributable mortality for the GLENS control scenario, which follows RCP8.5 forcings, and the feedback scenario, which adds SG to maintain multiple temperature targets at 2020 levels. For the RCP 8.5 scenario, global mortality risk increases convexly over the century (Figure 4). By the end of the century (2090–2097), it increases by 170 deaths per 100,000 per year relative to the reference period (2010–2019). When warming is offset with SG, we find that global mortality risk is instead reduced by an average of 0.36 deaths per 100,000 per year relative to the reference period.

Figure 4. Change in Temperature-Attributable Mortality for GLENS Climate Simulation

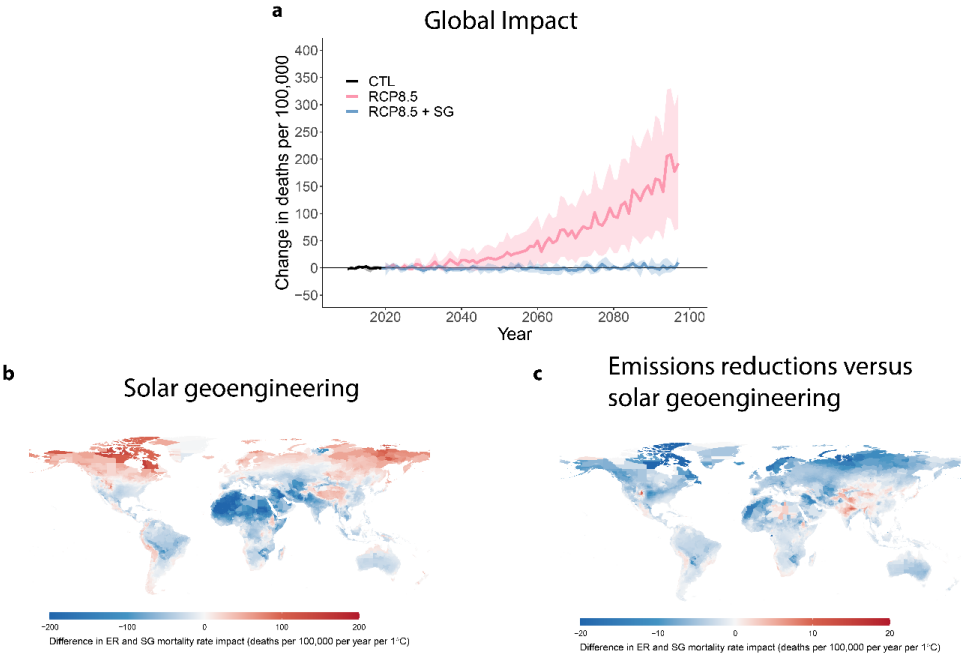

d

Impact of Solar Geoengineering								
	Decade							
Measure	2021-2029	2030-2039	2040-2049	2050-2059	2060-2069	2070-2079	2080-2089	2090-2097
$\Delta\bar{T}$ (°C)	0.2	0.7	1.4	2.2	2.7	3.3	4	4.8
SG (per 1°C)	0.1	8	12	14	22	24	30	36
r	1.14	1.03	1.2	1.09	1.18	1.09	1.06	1.04

Note: Change in temperature-attributable mortality for RCP8.5 scenario and RCP8.5 with solar geoengineering (SG). (a) All temperature-attributable mortality. Lines show median estimate and shading shows 10–90th percentile range of Monte Carlo simulations. (b) median estimates of regional mortality risk impact of SG normalized per degree of global mean cooling (2090–2097). (c) median estimates of difference in regional mortality risk impact of between emissions reductions and SG normalized per degree of global mean cooling (2090–2097). (d) Decadal effect of SG on global mean temperature, impact of SG on mortality normalized per degree of cooling, and ratio of normalized impact of SG relative to emissions reduction.

For more direct comparison of SG's impact, we can again normalize by the change in global mean cooling. Figure 4d shows this by decade. The impact on global average temperature-attributable mortality for the GLENS simulations is comparable to the results in the FLOR model for early- to midcentury. The increasing normalized impact over the century with more warming reflects the underlying convexity of the relationship.

We again compare the impact of SG to emissions reductions per degree of global cooling. Figure 4d shows estimates of the ratio r_M by decade. Our estimates of r_M over the century have some variation that likely reflects underlying variability, but throughout the century, we consistently find $r_M > 1$. Although GLENS adjusts the latitudinal distribution of injection to better manage the change in the pole–equator gradient, SG still reduces temperature-attributable mortality by more than emissions reductions per degree of global mean cooling.

4. Toward a Risk-Risk Comparison

SG can moderate the temperature-attributable mortality risk of climate change but also introduces novel risks. Recent research on SG has highlighted the urgent need for comparison of the risks as a guide for climate policy decisionmaking (Harding et al. 2022; Felgenhauer et al. 2022; Parson 2021; Aldy et al. 2021). Having quantified the benefits in terms of temperature-attributable mortality, we can compare them to the direct human mortality risk from sulfate aerosol geoengineering, which is a small but important step toward a more comprehensive quantitative risk–risk assessment.

SG through sulphate aerosol injection will cause changes in ozone, UV-B exposure, and particulate matter exposure. Previous estimates find that these changes will increase net mortality risk by an estimated 26,000 deaths per year (95 percent CI - 30,000–79,000), which offsets global mean temperature by 1°C in 2040 (Eastham 2018).[1] For a global population of seven billion, this is around 0.3 deaths per 100,000 per year per 1°C. We estimate a benefit of reduced mortality of around 17 deaths per 100,000 per year per 1°C. Across our robustness analyses, we find uncertainties are around order unity, with a low estimate of 9 deaths per 100,000 per year per 1°C and a high estimate of 36 for cooling of at least 0.5°C. This indicates that the benefits through reduced temperature-attributable mortality risk are at least 10x and as much as 100x the direct mortality risk of the aerosols used. This compares only two risk components, but these are plausibly two of the largest human mortality risk components.

5. Discussion

Human mortality risk from extreme weather is a major component of climate risk. We find that, SG could substantially reduce temperature-attributable mortality risk and may moderate this risk more than emissions reductions for equivalent global cooling. This is due to differences in the climate response between SG and emissions reductions, particularly a reduction in intra-annual temperature variability and relative cooling of the most sensitive equatorial regions. There is regional heterogeneity. Broadly, regions in the Global South tend to benefit from cooling, and risk increases in regions in the Global North. Our results are robust to a variety of alternative assumptions about socioeconomics, adaptation, and climate modeling.

Emissions cause long-term climate and geochemical risks that SG cannot abate, so it cannot substitute for emissions reductions. Our results do suggest that it could

[1] Of this total mortality risk, 10,000 deaths per year are attributable to the direct effects of adding SO_2 and 16,000 deaths per year are attributable to the changes in radiative forcing. The direct effects are unique to solar geoengineering, but the consequences of radiative forcing changes would plausibly still hold for any cooling.

supplement emissions reductions by moderating an important impact of climate change on human mortality and that the countervailing mortality risks examined are comparatively small.

Our work is just a step toward a broad quantitative risk–risk assessment of SG. We caution that quantitative risk–risk assessment cannot capture many important concerns about SG, so a favorable risk–risk ratio cannot serve as a sufficient justification for decisions about deployment.

6. Methods

6.1. FLOR

The model uses a high-resolution (50km) atmosphere and land component taken from the Coupled Model, v.2.5 (CM2.5) and a lower-resolution (1°) ocean and sea ice complement taken from the Coupled Model, v.2.1 (CM2.1) (see Vecchi et al. 2014 for full details of the model).

For FLOR, a control simulation is run for 300 years with conditions of 1990. The $2xCO_2$ experiment and solar dimming experiments branch off the control simulation in year 101 and run for 200 years. In the $2xCO_2$ experiment, atmospheric concentrations of CO_2 are doubled from the control simulation. In the solar dimming experiment, atmospheric concentrations of CO_2 are doubled from the control simulation and the solar constant is reduced by 1.7 percent. We use the last 100 years of each simulation for our analyses.

6.2. GLENS

The GLENS simulations are modeled using the NCAR Community Earth System Model, v.1 (CESM1), with the WACCM for the atmosphere component (see Tilmes et al. 2018 for full details of the simulations).

The control simulations use the greenhouse gas forcing concentrations for RCP 8.5 from 2010–2099. The SG simulations use RCP 8.5 concentrations with SO_2 injection at four latitudes—30N, 30S, 15N, and 15S—beginning in 2020. Aerosol injection is adjusted following a feedback-control algorithm to simultaneously minimize deviations in global mean surface temperature, interhemispheric temperature gradient, and the equator–pole temperature gradient from 2020 values. For our analyses, we use the three control and corresponding SG ensemble members that run to the end of the century.

6.3. Normalization

Throughout the analysis, we normalize climate response and mortality risk impacts by the change in global annual mean temperature. For example, the normalized response of a given variable X to solar geoengineering is given as

$$< X^{2xCO_2} - X^{SG} > = \frac{X^{2xCO_2} - X^{SG}}{\bar{T}^{2xCO_2} - \bar{T}^{SG}}$$

where $\bar{T}$ is the global annual mean temperature. This captures the change in the variable X per degree of global mean temperature cooling from SG. This is equivalent to linearizing the response of variable X to the change in global annual mean temperature. This can be calculated for changes in X at the grid-cell level or globally.

From this normalization, we introduce a ratio metric r to compare the effects of SG and emissions reductions. For a given variable X, the ratio r_X is given as

$$r_X = \frac{<X^{2xCO2} - X^{SG}>}{<X^{2xCO2} - X^{CTL}>}.$$

The ratio metric can also be calculated either at the grid-cell level or globally. The accuracy of this normalization and ratio approach depends on the assumption that responses are approximately linear in the change in global mean surface temperature. We do not test this assumption here, but it is found to be valid for a range of climate variables in other settings (Kravitz et al. 2014).

6.4. Empirical Estimated Impact

Temperature-attributable mortality risk estimates follow the methodology outlined in Carleton et al. (2022). We describe the key estimation methods for our setting. For a more comprehensive description see Carleton et al. (2022). We use the 24,378 impact regions, each around the size of a US county, and the corresponding calibrated SSP income and population data constructed in their analysis.

We estimate mortality impacts for each simulation year by integrating region- and age-specific dose–response curves—which describe the relationship between temperature and mortality rates—over daily temperatures. The curves are constructed using the estimates of the historical temperature–mortality relationship from Carleton et al. (2022), which relate mortality rates to temperature interacted with regions' climate and income, captured by their Equation (4) in their text.

For our baseline estimates, we fix the income covariate as the Bartlett kernel of income for SSP3 in 2015 with a length of 13 years. For the GFDL FLOR climate simulations, we fix the climate covariate as the average of annual mean temperature for the last 100 control simulation years. For GLENS climate simulations, we fix the climate covariate as the Bartlett kernel of annual mean temperature in 2015 with a length of 30 years. To analyze the effect of income growth, we alternatively use the Bartlett kernel of income for SSP3 in 2080. To analyze the effect of climate

adaptation, for the FLOR climate simulations, we use the average of annual mean temperature for the last 100 simulation years in each respective experiment. We do not account for adaptation costs for these projections. For the GLENS climate simulations, we allow the Bartlett kernel of annual mean temperature to evolve over time and account for the cost of adaptation following the method outlined in Carleton et al. (2022). For the FLOR model, impacts are aggregated using population weights for the SSP3 scenario in 2080, a more realistic year for SG to be implemented with a 1°C magnitude. For the GLENS model, impacts are aggregated using population weights for the SSP3 scenario in each respective year.

We account for uncertainty in both the econometric estimates and the climate simulations using Monte Carlo simulations. To account for econometric uncertainty, we randomly sample coefficients for the econometric parameters using a multivariate normal distribution characterized by the covariance matrix between all the parameters. To account for climate uncertainty in the FLOR model we randomly draw simulation years. To account for climate uncertainty in the GLENS simulations, we randomly draw ensemble members. This process of randomly drawing a set of coefficients and a model year or an ensemble member is repeated 1,000 times.

6.5. Downscaling and Bias Correction

To mitigate concerns of stationary biases (Auffhammer 2013) in our empirical analysis of temperature-attributable mortality, we downscale and bias-correct both the FLOR and GLENS climate simulation output. First, minimum and maximum daily 2m temperature are downscaled to a 0.25°x0.25° spatial resolution using bilinear interpolation. Next, downscaled temperature is bias corrected to the GMFD data (Sheffield et al. 2006) used to empirically estimate historical dose–response functions. Data are bias corrected following the ISI-MIP method (Hempel 2013). For the FLOR, the first 10 years of the control scenario is matched to the GMFD data for 1990–1999 because the control is set to 1990s conditions. For the GLENS model, 1980–2010 are matched to the corresponding years in the GMFD data. Finally, we calculate daily average temperature for each of the impact regions as the population-weighted mean of daily maximum and minimum temperature. Population weights come from LandScan Global 2011 (Bright 2012).

6.6. WBT and WGBT

WBT (T_w) is calculated as a function of ambient temperature (T_a) and relative humidity ($RH\%$) using the following approximating formula developed by Stull (2011):

$$\begin{aligned} T_w = \; & T_a \operatorname{atan}\left[0.151977(RH\% + 8.313659)^{\frac{1}{2}}\right] + \operatorname{atan}(T_a + RH\%) \\ & - \operatorname{atan}(RH\% - 1.676331) \\ & + 0.00391838(RH\%)^{\frac{3}{2}}\operatorname{atan}(0.023101RH\%) - 4.686035 \end{aligned}$$

This formula is accurate for relative humidity of 5–99 percent and ambient temperature of -20C–50C, except for both low humidity and cold temperature.

WBGT is a linear combination of ambient temperature ($\mathrm{T_a}$), natural WBT ($\mathrm{T_w}$), and black globe temperature ($\mathrm{T_g}$), given as

$$\mathrm{WBGT} = 0.1\mathrm{T_a} + 0.7\mathrm{T_w} + 0.2\mathrm{T_g}$$

To calculate WBGT, we follow the model of Liljegren et al. (2008) using code developed by Kong and Huber (2022).

7. References

Aldy, J., et al. 2021. Social Science Research to Inform Solar Geoengineering. *Science* 374: 815–8.

Auffhammer, M., S.M. Hsiang, W. Schlenker, and A. Sobel. 2013. Using Weather Data and Climate Model Output in Economic Analyses of Climate Change. *Review of Environmental Economics and Policy* 7: 181–98.

Buzan, J.R., and M. Huber. 2020. Moist Heat Stress on a Hotter Earth. *Annual Review of Earth and Planetary Sciences Sci.* 48: 623–55.

Ban-Weiss, G. A., and K. Caldeira. 2010. Geoengineering as an Optimization Problem. *Environmental Resource Letters* 5: 034009.

Bednarz, E. M., et al. 2022. The Overlooked Role of the Stratosphere Under a Solar Constant Reduction. *Geophysical Resource Letters* 49: e2022GL098773.

Bright, E., P. Coleman, A. Rose, and M. Urban. 2012. "LandScan Global 2011." [doi: 10.48690/1524207]

Carleton, T. et al. 2022. "Valuing the global mortality consequences of climate change accounting for adaptation costs and benefits." *Quarterly Journal of Economics* 137(4): 2037–2105. [doi: 10.1093/qje/qjac020]

Carlson, C.J., et al. 2022. Solar Geoengineering Could Redistribute Malaria Risk in Developing Countries. *Nature Communications* 13: 2150.

Chen, Y., A. Liu, and J.C. Moore. 2020. Mitigation of Arctic Permafrost Carbon Loss Through Stratospheric Aerosol Geoengineering. *Nature Communications* 11: 1–10.

Chen, Y., et al. 2022. Northern High-Latitude Permafrost and Terrestrial Carbon Response to Solar Geoengineering. *Earth Systems Dynamic Discussion*: 1–39.

Dagon, K., and D.P. Schrag. 2017. Regional Climate Variability Under Model Simulations of Solar Geoengineering. *Journal of Geophysical Research: Atmospheres* 122(12): 106–12.

Eastham, S.D., D.K. Weisenstein, David W. Keith, and S.R.H. Barrett. 2018. Quantifying the Impact of Sulfate Geoengineering on Mortality from Air Quality and UV-B Exposure. *Atmosphere Environment* 187: 424–434.

Fan, Y., et al. 2021. Solar Geoengineering Can Alleviate Climate Change Pressures on Crop Yields. *Nat. Food* 2: 373–381.

Felgenhauer, T. et al. 2022. *Solar Radiation Modification: A Risk–Risk Analysis*. **https://scholars.duke.edu/display/pub1508823**.

Govindasamy, B., and K. Caldeira. 2000. Geoengineering Earth's Radiation Balance to Mitigate CO_2-Induced Climate Change. *Geophysical Resource Letters*. 27: 2141–44.

Harding, A. R., M. Belaia, and David W. Keith. 2022. The Value of Information About Solar Geoengineering and the Two-Sided Cost of Bias. *Climate Policy* 1: 1–11.

Harding, A.R., K. Ricke, D. Heyen, D.G. MacMartin, and J. Moreno-Cruz. 2020. Climate Econometric Models Indicate Solar Geoengineering Would Reduce Inter-Country Income Inequality. *Nature Communications* 11: 227.

Hempel, S., K. Frieler, L. Warszawski, J. Schewe, and F. Piontek. 2013. A Trend-Preserving Bias Correction—the ISI-MIP Approach. *Earth System Dynamics* 4: 219–36.

ICC (Interagency Working Group on Social Cost of Greenhouse Gases, United States Government). 2021. *Technical Support Document: Social Cost of Carbon, Methane, and Nitrous Oxide Interim Estimates Under Executive Order 13990*.

Irvine, P.J., and David W. Keith. 2020. Halving Warming with Stratospheric Aerosol Geoengineering Moderates Policy-Relevant Climate Hazards. *Environmental Resource Letters* 15, 044011.

Irvine, P.J., B. Kravitz, M.G. Lawrence, and H., Muri. 2016. An Overview of the Earth System Science of Solar Geoengineering. *Wiley Interdisciplinary Reviews: Climatic Change* 7: 815–33.

Kong, Q., and M. Huber. 2022. Explicit Calculations of Wet-Bulb Globe Temperature Compared With Approximations and Why It Matters for Labor Productivity. *Earth's Future* 10: e2021EF002334.

Kravitz, B., et al. 2014. A Multi-Model Assessment of Regional Climate Disparities Caused By Solar Geoengineering. *Environmental Resource Letters* 9: 074013.

Kravitz, B., et al. 2019. Comparing Surface and Stratospheric Impacts of Geoengineering With Different SO_2 Injection Strategies. *Journal of Geophysical Research: Atmospheres* 124: 7900–18.

Kuswanto, H., et al. 2022. Impact of Solar Geoengineering on Temperatures Over the Indonesian Maritime Continent. *International Journal of Climatology* 42: 2795–2814.

Liljegren, J.C., R.A. Carhart, P. Lawday, S. Tschopp, and R. Sharp. 2008. Modeling the Wet Bulb Globe Temperature Using Standard Meteorological Measurements. *Journal of Occupational and Environmental Hygiene* 5: 645–55.

Moreno-Cruz, J.B., K.L. Ricke, and David W. Keith. 2012. A Simple Model to Account for Regional Inequalities in the Effectiveness of Solar Radiation Management. *Climatic Change* 110: 649–68.

Parker, A., and P.J. Irvine. 2018. The Risk of Termination Shock From Solar Geoengineering. *Earth's Future* 6: 456–67.

Parson, E. A. 2021. Geoengineering: Symmetric Precaution. *Science* 374: 795.

Philip, S. Y., et al. 2021. "Rapid attribution analysis of the extraordinary heatwave on the Pacific Coast of the US and Canada June 2021." *Earth Systems Dynamic Discussion*: 1–34 [doi: 10.5194/esd-2021-90]

Rennert, K., et al. 2020. "Comprehensive evidence implies a higher social cost of CO_2." *Nature* 1–3 [doi: 10.1038/s41586-022-05224-9]

Stull, R. 2011. Wet-Bulb Temperature from Relative Humidity and Air Temperature. *Journal Applied Meteorology and Climatology* 50: 2267–69.

Tilmes, S., et al. 2018. CESM1(WACCM) Stratospheric Aerosol Geoengineering Large Ensemble Project. *Bulletin of the American Meteorological Society* 99: 2361–71.

UN (United Nations) Department of Economic and Social Affairs, Population Division. 2022. *World Population Prospects: The 2022 Revision*. United Nations Department of Economic and Social Affairs, Population Division.

Van der Wiel, K., et al. 2016. The Resolution Dependence of Contiguous US Precipitation Extremes in Response to CO_2 Forcing. *Journal of Climate* 29: 7991–8012.

Vecchi, G. A., et al. 2014. On the Seasonal Forecasting of Regional Tropical Cyclone Activity. *Journal of Climate* 27: 7994–8016.

Visioni, D., D.G. MacMartin, and B. Kravitz. 2021. Is Turning Down the Sun a Good Proxy for Stratospheric Sulfate Geoengineering? *Journal of Geophysical Research: Atmospheres* 126: e2020JD033952.

Figure ED1. Empirical Dose–Response Function

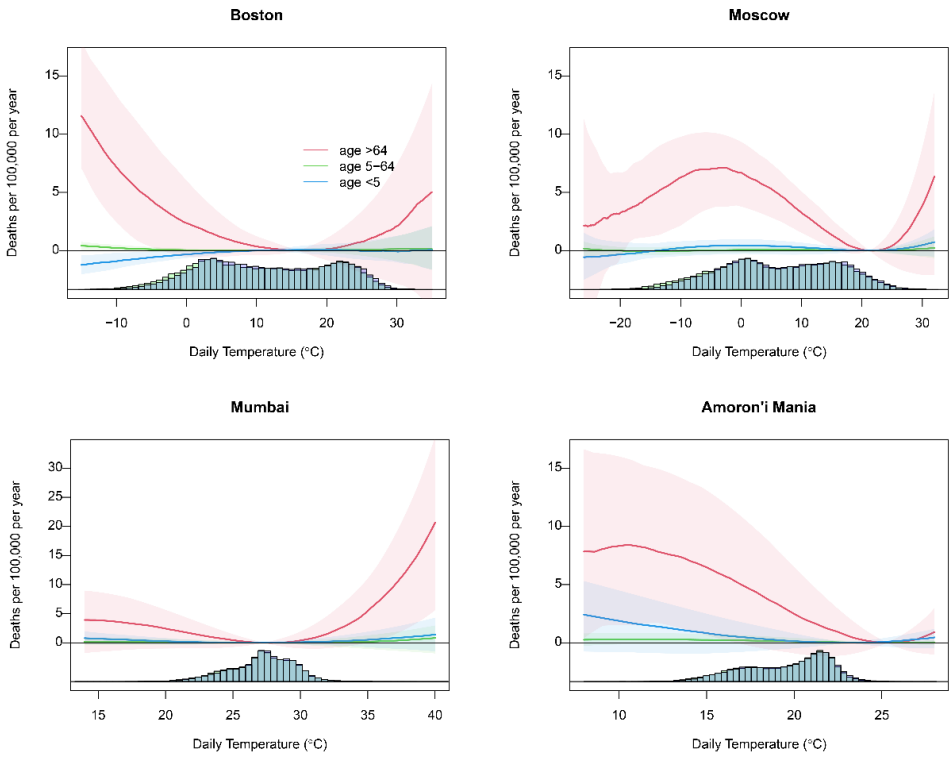

Note: Temperature–mortality dose–response function for four regions and the distribution of daily temperatures in each region. Plotted for climate and income in 2015 without clipping. Line indicates median estimate. Shading indicates 95 percent CIs.

Figure ED2. Uncertainty in mortality impact

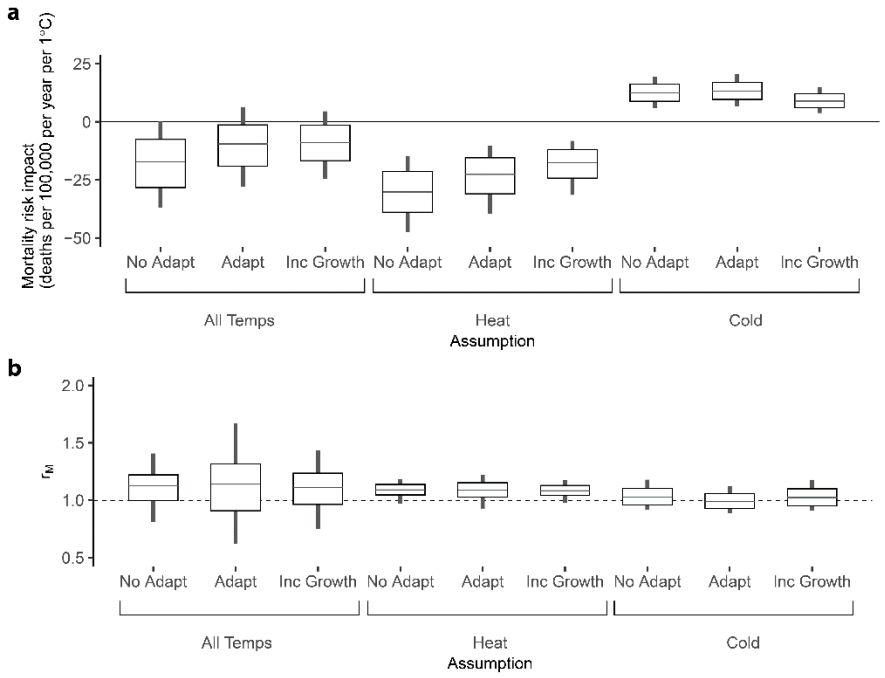

Note: **(a)** Global mortality risk impact of solar geoengineering (SG) normalized per degree of global mean cooling for all temperature-attributable mortality, heat-attributable mortality, and cold-attributable mortality across different modeling assumptions. **(b)** Ratio of global mortality risk impact for SG relative to emissions reductions normalized per degree of global mean cooling for all temperature-attributable, heat-attributable, and cold-attributable mortality across different modeling assumptions. Lines represent median estimates, boxes capture interquartile range, and lines extend to the 10th and 90th percentiles of Monte Carlo simulations.

Figure ED3. Mortality risk impact by income decile

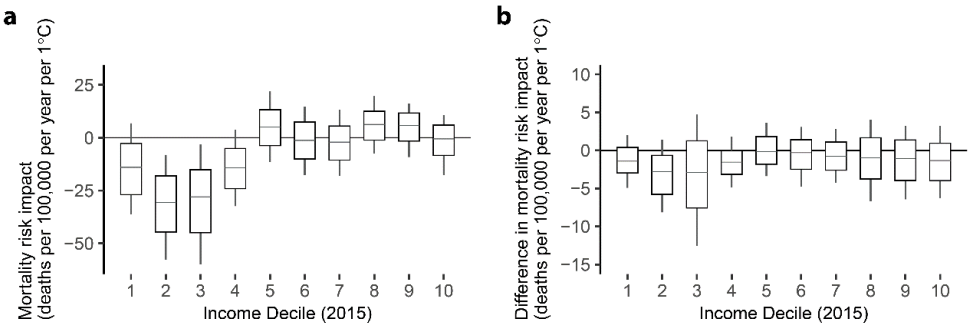

Note: **(a)** Mortality risk impact of solar geoengineering (SG) normalized per degree of global mean cooling by income decile. **(b)** Difference in mortality risk impact normalized per degree of global mean cooling between emissions reductions and SG by income decile, defined using SSP3 income in 2015. Lines represent median estimates, boxes capture interquartile range, and lines extend to 10th and 90th percentiles of Monte Carlo simulations.

Figure ED4. Difference in heat- and cold-attributable mortality risk impact

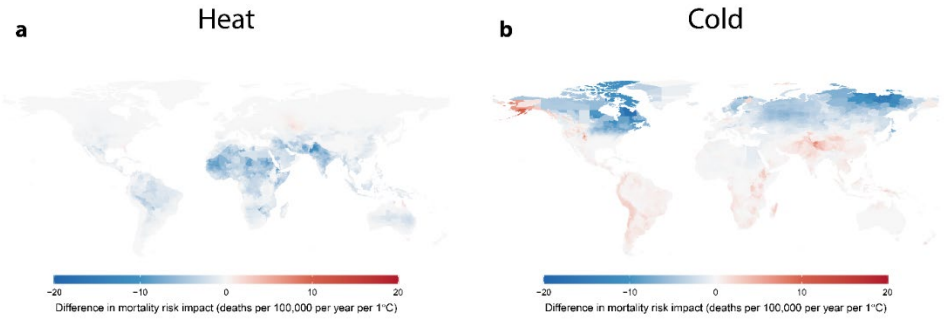

Note: Difference in mortality risk impact normalized per degree of global mean cooling between concentration reductions and solar geoengineering for **(a)** heat-attributable and **(b)** cold-attributable mortality risk.